Response of high speed EDS maglev train moving on a suspended guideway shaken by horizontal earthquake

J.D. Yau
Department of Architecture
Tamkang University
No.151, Yingzhuan Rd., Tamsui Dist., New Taipei City 25137
TAIWAN
jdyau@mail.tku.edu.tw

Abstract: - This paper presented a computational framework of interaction analysis for an EDS (electro-dynamic suspension) maglev train traveling over a suspension bridge shaken by horizontal earthquakes. The suspended guideway girder is modeled as a single-span suspended beam and the maglev train traveling over it as a series of maglev masses. To tune the magnetic forces in a maglev suspension system, an on-board hybrid LQR+PID controller is designed to control the dynamic response of a running maglev mass. Then the governing equations of motion for the suspended beam associated with all the controlled maglev masses are transformed into a set of generalized equations by Galerkin's method, and solved using an incremental-iterative procedure. Numerical investigations demonstrate that when a controlled maglev train travels over a suspended guideway shaken by horizontal earthquakes, the proposed hybrid controller has ability to reduce the vehicle's acceleration response for ride quality.

Key-Words: - maglev system; earthquake; iterative-incremental method; suspended guideway.

1 Introduction

In the past one decade, various dynamic interaction models of maglev/guideway coupled system were developed by the researchers from different countries. Most of them focused on the vibration of a maglev vehicle running on a flexible guideway system [1-5]. Cai and Chen [1] provided a literature review for various aspects of the dynamic characteristics, magnetic suspension systems, vehicle stability, suspension control laws of maglev/guideway coupling systems. Concerning the interaction response of a maglev train traveling over a flexible guideway girder, Cai et al. [2] pointed out that a concentrated-load vehicle model would result in larger response on the vehicle/guideway system than a distributed-load one. Zheng *et al*. [3,4] developed two kinds of vehicle/guideway coupling models with controllable magnetic suspension systems to observe the phenomena of divergence, flutter, and collision on the dynamic stability of a maglev-vehicle traveling on a flexible guideway. Zhao and Zhai [5] simulated a TR06 carriage as a ten-degree-of-freedom (10-dof) rigid vehicle model to investigate the ride quality of a maglev vehicle traveling on elevated guideways. In the latest study, Yau [6,7] proposed an on-board PI controller to control the interaction response of a maglev vehicle running on flexible guideways by using an incremental-iterative procedure. However, rather limited research works seem available to conduct the influence of seismic ground motion on interaction behaviour of a maglev train crossing a suspended guideway..

The objective of this study is to present a computational framework of interaction analysis using an incremental-iterative procedure to compute the dynamic response of a *controlled* maglev train travelling over a suspended guideway shaken by horizontal earthquakes. Control of levitation forces between the magnet and guide-rail requires the guideway clearance be continuously monitored. Thus a hybrid LQR+PID controller is designed to meet the performance criteria of desired workable air gaps and restricted acceleration amplitudes for a running maglev vehicle. Considering the shaking effect of horizontal ground motion, the coupled equations of motion for maglev vehicle/guideway system are formulated using a dynamic interaction model of a single-span suspended beam carrying multiple moving maglev masses. Then the governing equations of motion for the suspended beam associated with all the controlled maglev masses are transformed into a set of generalized equations by Galerkin's method and solved by the Newmark method in the time domain.

From the numerical results, although the inclusion of horizontal seismic ground motion may result in a significant amplification on both dynamic responses of the vehicle/guideway interaction system, the proposed hybrid controller has the ability to achieve the performance criteria of travelling safety and ride quality through continuous air-gap monitoring and sustaining acceleration adjustment.
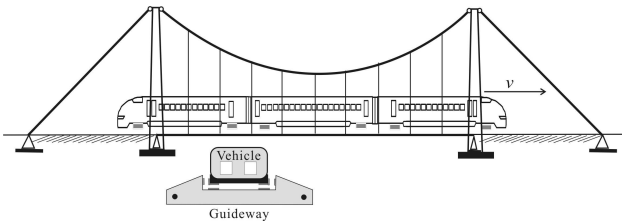

Fig. 1 Suspended guideway traveled by a maglev train.

2 Problem Formulation

Figure 1 shows a schematic diagram for an EDS maglev train running on a suspended guideway. This study will model a maglev train as a series of maglev masses and focus on the *vertical* response of the maglev masses traveling over a single-span suspended guidedway. Based on the *deflection theory* [8,9] that can take into account the additional cable tension of a suspended beam due to live loads, appreciable simplifications for the suspended guideway and maglev vehicles are outlined as follows:

(1) the suspended guideway girder is modeled as a linear elastic Bernoulli-Euler beam with uniform cross section;

(2) as shown in Fig. 2, the bridge towers are assumed so rigid that their deformations are negligible;

(3) the suspension cable can carry all the dead loads of the stiffening girder with the aid of inextensible vertical hangers so that the suspended beam is in an un-stressed state before the action of live loads;

(4) the maglev train passing over the suspended beam is simulated as a sequence of moving maglev masses with regular intervals;

(5) only the horizontal ground motion in longitudinal direction along the guideway is considered;

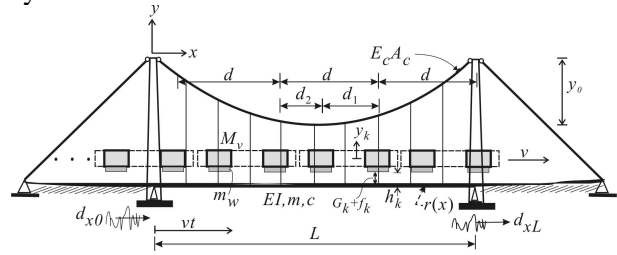(6) there is no time delay between the input voltage and output current in the maglev suspension system.

Fig. 2 Model of a series of maglev masses running on a suspended beam.

2.1 Governing equations

Based on the *deflection theory* for small deformations of suspension bridges [8,9], the equation of vertical motion for a suspended beam carrying multiple moving maglev masses is given by:

$$m\ddot{u} + c\dot{u} + EIu'''' - (T + \Delta T)(y'' + u'') = w + p(x,t)$$

$$p(x,t) = -\sum_{k=1}^{K} [G_k(i_k, h_k) + f_k]\varphi(x,t) \times \delta(x - x_k),$$

$$\varphi(x,t) = H(t - t_g - t_k) - H(t - t_g - t_k - L/v),$$

(1)

where $(\bullet)' = \partial(\bullet)/\partial x$, $(\dot{\bullet}) = \partial(\bullet)/\partial t$, m = mass of the beam and cable per unit length along x-axis, c = damping coefficient, f_k = additional control force induced by a hybrid controller, G_k = control magnetic force, i_k = control current, h_k = levitation gap, $u(x,t)$ = vertical deflection of the beam, EI = flexural rigidity of the beam, T = horizontal component in the initial cable tension (due to dead loads), ΔT = additional horizontal component in cable force due to external loads, $\delta(\bullet)$ = Dirac's delta function, $H(t)$ = unit step function, t_k = arrival time of the kth maglev mass into the beam, $k = 1, 2, 3, \ldots, K$th moving maglev mass on the suspended beam, t_g = time lag for the first maglev mass entering the suspended beam, and $p(x,t)$ = loading function of moving maglev masses. Consider the shaking effect of horizontal seismic support motion acting on the rigid bridge towers shown in Fig. 2, the time-dependent boundary conditions for the suspended beam with hinged ends are given by:

$$u_x(0,t) = d_{x0}(t), u_x(L,t) = d_{xL}(t),$$

$$u(0,t) = 0, u(L,t) = 0; EIu''(0,t) = EIu''(L,t) = 0,$$

(2)

where (d_{x0}, d_{xL}) represent the horizontal support movements at the left and right bridge towers, respectively. By including the horizontal support movements, an additional horizontal component ΔT in the cable due to external excitation is equal to[25]

$$\Delta T = \frac{E_c A_c}{L_c}\left[(d_{xL} - d_{x0}) + \frac{8y_0}{L^2}\int_0^L u\, dx \right],$$

(3)

in which E_c = elastic modulus of the cable, A_c = area of the cable, and L_c = the effective length of the cable. Substituting Eq. (3) into Eq. (1) yields the following equation of motion for a suspended beam under the simultaneous action of multiple moving maglev masses and horizontal support movements

$$m\ddot{u} + c\dot{u} + EIu'''' - (T + \Delta T_s)u'' + (\alpha + \kappa u'')\int_0^L u dx \qquad (4)$$
$$= p(x,t) - \kappa(d_{xL} - d_{x0}),$$

with

$$\alpha = \left(\frac{8y_0}{L^2}\right)^2 \frac{E_c A_c}{L_c}, \kappa = \left(\frac{8y_0}{L^2}\right)\frac{E_c A_c}{L_c}. \qquad (5)$$

As shown in Eq. (4), the horizontal ground motion may affect the vertical vibration of a suspended beam through multiple support movements, that is, $d_{x0} \neq d_{xL}$. Since the increment of horizontal component of cable force in Eq. (3) is dependent on both the beam deflection $u(x,t)$ and horizontal support movements (d_{x0}, d_{xL}), the integro-differential equation of motion in Eq. (4) is non-linear in nature because of the presence of ΔT_s .

2.2 Control equation of the maglev system

The control equation of the maglev mass with LQR control algorithm is given by [8]:

$$M\ddot{y}_k + \rho_2\dot{y}_k + \rho_1 y_k = G_k(i_k, h_k) - p_0, \qquad (6)$$

with

$$\rho_1 = \sqrt{k_b/R}, \rho_2 = \sqrt{M\left(2\sqrt{k_b/R} + 1/R\right)}. \qquad (7)$$

and R the weighting parameter for the input control force. Observing the term $1/R$ in Eq. (19), it indicates that if R approaches to a very large value, i.e., $1/R \to 0$, Eq. (20) is reduced to the initial equation of motion with less input control gains to the controlled maglev mass. Moreover, the designer may select a pair of suitable stiffness and damping coefficients to reduce the vehicle's response to various degrees by trying different combinations of weighting parameters (k_b, R).

By the theory of electromagnetic circuits, the electromagnetic equation of magnet current and control voltage for the kth magnetic wheel in the magnetic suspension system is given by [8]

$$\Gamma_0 \frac{d(i_k/h_k)}{dt} + R_0 i_k = V_k, \qquad (8)$$

where $\Gamma_0 = 2\kappa_0$ = initial inductance of the coil winding the suspension magnet, R_0 = coil resistance of electronic circuit, and V_k = control voltage. To conduct the dynamic response of mgalev vehicle/guideway system subject to ground settlement, an on-board PI controller with *constant* tuning gains is employed for the moving maglev vehicle. On the other hand, the control voltage V_k

can be expressed using PID tuning algorithm as [11-13]

$$V_k = K_d \dot{e}_k + K_p e_k + K_i \int_0^t e_k dt, \qquad (9)$$

where K_d = derivative gain, K_p = proportional gain and K_i = integral gain. Let us adopt the variable transformation as $\gamma_k = i_k/h_k$, and the error function of $e_k = i_0/h_0 - i_k/h_k = \gamma_0 - \gamma_k$ in the control process. Then substituting Eq. (9) into Eq. (8) and differentiating this equation with respect to time, after some mathematical manipulation, one can achieve the following differential equation for control error function

$$(\Gamma_0 + K_d)\ddot{e}_k + (K_p + R_0 h_k)\dot{e}_k + (K_i + R_0 \dot{h}_k)e_k \qquad (10)$$
$$- R_0\gamma_0\dot{y}_k = -R_0\gamma_0(\dot{u} - \dot{r})\big|_{x = x_k} .$$

With the aid of control error function e_k and $\gamma_0 = i_0/h_0$ defined previously, the equations of motion in Eqs. (3) and (4) for the kth maglev mass equipped with an on-board hybrid LQR+PID controller are rewritten

$$[m_{v,k}]\{\ddot{u}_{v,k}\} + [c_{v,k}]\{\dot{u}_{v,k}\} + [k_{v,k}]\{u_{v,k}\} = \{f_{v,k}\}, \qquad (11)$$

of which the displacement vector $\{u_{v,k}\}$, force vector $\{f_{v,k}\}$, and structural matrices of $[k_{v,k}]$, $[c_{v,k}]$, and $[m_{v,k}]$ are given as follows:

$$\{u_{v,k}\} = \begin{Bmatrix} y_k \\ e_k \end{Bmatrix}, [m_{v,k}] = \begin{bmatrix} M & 0 \\ 0 & K_d + \Gamma_0 \end{bmatrix},$$

$$[c_{v,k}] = \begin{bmatrix} \rho_2 & 0 \\ -R_0\gamma_0 & K_p + R_0 h_k \end{bmatrix}, \qquad (12)$$

$$[k_{v,k}] = \begin{bmatrix} \rho_1 & 2p_0/\gamma_0 \\ 0 & K_i + R_0 \dot{h}_k \end{bmatrix}, \{f_{v,k}\} = \begin{Bmatrix} p_0 \times e_k^2/\gamma_0^2 \\ -R_0\gamma_0(\dot{u} - \dot{r})\big|_{x = x_k} \end{Bmatrix}.$$

3 Problem Solution

According to the homogeneous boundary conditions shown in Eq. (2), the dynamic deflection of the suspended beam can be approximated by:

$$u(x,t) = \sum_{n=1} q_n(t)\sin\frac{n\pi x}{L} \qquad (13)$$

where $q_n(t)$ means the generalized coordinate associated with the nth assumed mode of the suspended beam. By Galerkin's method, one can transform the equation of motion for the suspended beam in Eq. (4) into the following generalized system equations. Then, the nth generalized equation of motion of the suspended beam is:

$$m\ddot{q}_n + c\dot{q}_n + \left(\frac{n\pi}{L}\right)^2\left[\left(\frac{n\pi}{L}\right)^2 EI + (T + \Delta T_s)\right]q_n + \Pi_n \qquad (14)$$

$$= p_n(t) - \frac{2\kappa}{n\pi}(1 - \cos(n\pi))(d_{xL} - d_{x0}),$$

where

$$\Pi_n = \frac{2\alpha L}{n\pi^2}(1-\cos n\pi)\left[\sum_k \frac{1}{k}(1-\cos k\pi)q_k\right], \qquad (15)$$

$$p_n(t) = -\frac{2}{L}\sum_{k=1}^{K}\left[(G_k(i_k,h_k)+f_k)\sin\varpi_n(t-t_k)\varphi(x,t)\right], \qquad (16)$$

with $\varpi_n = n\pi v/L$. It is noted that the generalized loading function $p_n(t)$ in Eq. (16) is related to the control levitation forces obtained from Section 2. For this reason, an iterative method has to be carried out for solving the dynamic response of the maglev mass/guideway coupling system.

4 Numerical Studies

Because of the motion-dependent nature of electromagnetic forces, the nonlinear dynamic analysis of the maglev vehicle/guideway system needs to be solved by iterative method. The procedure of incremental-iterative dynamic analysis conventionally involves three phases: *predictor*, *corrector,* and *equilibrium checking* [6]. Details concerning the incremental-iterative procedure for nonlinear dynamic analysis of vehicle-bridge interaction are available in Ref. [6].

Prior to investigating the dynamic response of the maglev vehicle/guideway system subject to horizontal ground motion, a TR06 maglev vehicle model referred to as Ref. [5] is selected to simulate its dynamic behavior running on a single-span concrete guideway girder with *smooth* surface. Let us represent the TR06 maglev vehicle as 8 lumped maglev masses with identical intervals ($d_1 = d_2 = 3$m) moving at constant speed of 400km/h [5]. The main data for the TR06 maglev vehicle model and the guideway girder [5] are given as follows: $EI = 24.56 \times 10^6$ kNm^2, $L = 24.854$m, $m = 3760$kg/m, $M = 7.6$t, $h_0 = 8$mm, $i_0 = 37$ampere(A), and $R_0 = 1.1$ohm(Ω).

As the schematic diagram of Fig. 2, a series of moving maglev masses (4 cars simulated by 8 lumped masses) are crossing a single-span suspended beam at constant speed v. The properties of the suspended beam and maglev mass unit are listed in Tables 1 and 2, respectively. In Table 1, the symbol of f_i represents the ith modal frequency of the suspended beam. Generally speaking, the acceleration response of vehicle-bridge system is usually used to evaluate the ride quality and manoeuvrability of high-speed ground transport system. In this study, the use of first 16 modes is considered sufficient to compute the dynamic response of a suspended beam under the action of multiple moving loads. For this reason, the same number of modes will be used in all the examples to follow. Moreover, as the *passage frequency* (= v/d)

of train loadings with regular interval (d) matches any of natural frequencies (f_i) of a bridge, the resonant response of the bridge will be developed [14,15], and the corresponding speed is denoted as $v_{res,i} = f_i d$. This is so called *resonance phenomenon* for train-induced response of railway bridges. In the following numerical examples, the levitation gap (h_k) of any of the moving maglev masses should be always positive for running safety.

.

Table 1. Properties of the suspended beam.

L (m)	EI (kN-m^2)	E_cA_c (kN)	m (t/m)	c (kN-s/m/m)	y_0 (m)	E_cA_c/L_e (kN/m)
80	2.96×10^7	1.6×10^7	5	1.88	8.8	1.82×10^5

Table 2. Properties of moving maglev mass

d	d_1 (m)	d_2 (m)	M_v (t)	m_w (t)	i_0 (A)	R_0 (Ω)
25	20	5	18	2	25	1.0

Table 3. PID optimal parameters based on the Z-N tuning method.

Type	h_0 (m)	K_{cr}	T_{cr} (s)	K_p	K_i	K_d
MG-1 / MG-2	0.15 / 0.10	1.2	0.31	0.72	4.65	0.047

4.1 Maximum acceleration response analysis

Let us use the optimal PID parameters listed in Table 3 to tune the control voltage of the maglev suspension system. By ranging the running speeds from 150km/h~350km/h with an increment of 5km/h, the computed maximum acceleration responses ($a_{v,max}$) of MG-1 and MG-2 against the speed (v) have been drawn in Fig. 3. Such a plot will be called $a_{v,max}$–v plot in the following examples. The numerical results indicate that the acceleration amplitude reaches its maximum value at the first resonant speed of 218km/h but is suppressed at the second resonant speed of 245km/h. One reason for this is that as a row of moving masses, with regular intervals of ($d_1 = 20$m, $d_2 = 5$m) far smaller than the guideway span ($L = 80$m), travel over a suspended beam, the simultaneous presence of multiple maglev masses on the guideway may produce a suppression action on the first symmetric bending mode (i.e., $\smile$), making the mid-span acceleration of the suspended guideway less severe compared with the first resonant case involving the anti-symmetric mode. Such a phenomenon can be observed in the following illustration. Consider the maximum acceleration response amplitude ($a_{b,max}$) along the
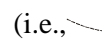
suspended beam (x/L) under the action of MG-1 and MG-2 moving with the first two resonant speeds, i.e., $v_{1,res}$ and $v_{2,res}$, respectively. The corresponding $a_{b,max}$–x/L plots have been drawn in Fig. 4. As can be seen from the resonant and sub-resonant peaks, the maximum acceleration response along the suspended beam with respect to the first two resonant speeds of 218 and 245km/h are governed by the anti-symmetrical and symmetrical modes, respectively. But the mid-span acceleration amplitude of the beam is significantly suppressed at the second resonant speed of 245km/h.
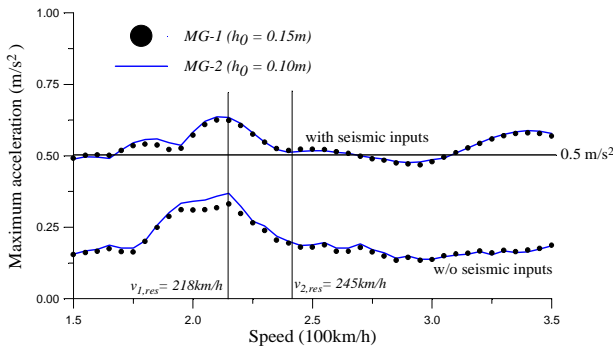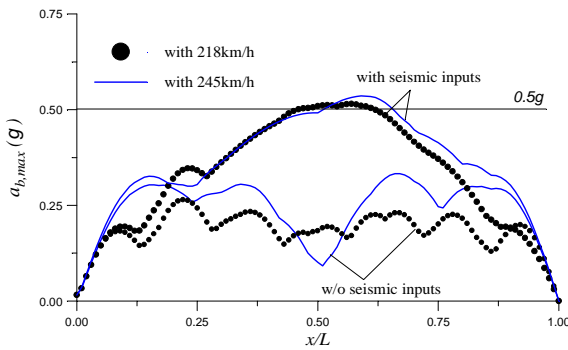

Fig. 3 $a_{v,max}$–v plot for the maglev masses.

Fig. 4 Seismic effect on $a_{b,max}$–x/L plot

4.2 Effect of horizontal ground motion
To investigate the influence of seismic ground motion on interaction response of maglev-vehicle/guideway system, the far-field ground motion recorded at free-field station (TAP003) during the 1999 Chi-Chi Earthquake in Taiwan [19] are used to simulate the seismic support inputs acting on the suspended guideway. The histogram of ground displacement containing the EW horizontal component has been plotted in Fig. 12. As can be seen, the intensive zone of horizontal ground movements appears nearby 25s. In order to let the rear part of the maglev masses moving on the suspended guideway has the possibility to experience the action of peak ground motions in the duration between 25s and 28s, the critical time of 25s is employed for the maglev train model to start entering the gudieway girder in the following

examples. Besides, suppose the bridge foundations are anchored to bedrock in a rock site with a seismic wave speed of 1000m/s and the ground motion at the right bridge support has a time lag of $L/1000$ (= 0.08s) behind the left one.
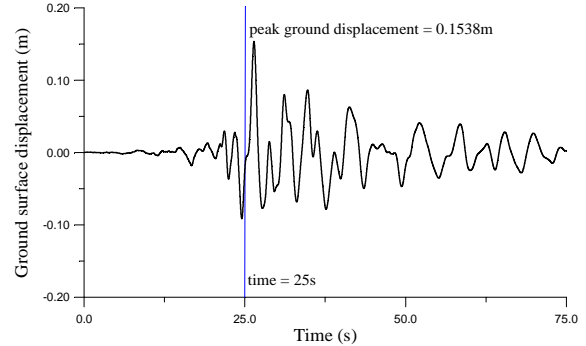

Fig. 5 Histogram of EW horizontal ground displacement of TAP003 Station.

Let us use the TAP003-EW seismic inputs shown in Fig. 5 to shake the suspended beam. The $a_{b,max}$–x/L plots with respect to the first two resonant speeds have been drawn in Fig. 4 as well, in which the maximum acceleration amplitudes are totally amplified and slightly greater than $0.5g$ (= 4.9m/s^2). Obviously, such excessive oscillations in the vibrating suspended beam will be feedback to the maglev mass system over it. The corresponding $a_{v,max}$–v plots for MG-1 and MG-2 have been depicted in Fig. 3 as well. As can be seen from the $a_{v,max}$–v plots denoted by "with seismic inputs", the maximum acceleration amplitudes of the maglev masses are totally amplified due to seismic wave passage effect.

From the present study, the $a_{v,max}$–v plots with seismic inputs in Fig. 3 indicate that most of which have exceeded the upper bound of coded acceleration amplitude of $0.05g$ (= 0.49 m/s^2) [5]. Besides, the vertical working air gap of the magnet motion in practice for a moving maglev vehicle should be restricted within a desired workable range. For this consideration, a further study will be carried out by adopting another control algorithm with constraint rules.

6 Conclusion
This paper presented an iteration-based computational procedure for maglev vehicle/guideway interaction system subjected to horizontal earthquake. From the numerical studies, the following conclusions are reached:
(1) The PID+LQR tuning algorithm incorporating with Z-N rule is available to control the

magnetic forces of a running maglev train.

(2) As the *passage frequencies* (*v/d*) caused by an EDS maglev train traveling over a suspended guideway girder coincides with any of the girder frequencies, resonance will be developed on the girder. Such a phenomenon has been observed from the $a_{b,max}$–x/L plots, in which higher modes are also excited.

(3) Because of the trait of large air gaps, an EDS-type maglev vehicle offers enough guideway clearance to accommodate additional vertical motion of the magnets induced by earthquakes. Thus the dynamic responses of both the maglev mass systems, MG-1 (h_0 = 0.15m) and MG-2 (h_0 = 0.1m), are quite close.

Acknowledgement

References:

[1] Y. Cai, S.S. Chen, D.M. Rote, H.T. Coffey, Vehicle/guideway dynamic interaction in maglev systems, Journal of Dynamic Systems, Measurement, and Control 118 (1996) 526–530.

[2] Y. Cai, S.S. Chen, Dynamic characteristics of magnetically-levitated vehicle systems, Applied Mechanics Reviews 50(11) (1997) 647–670.

[3] X.J. Zheng, J.J. Wu, Y.H. Zhou, Numerical analyses on dynamic control of five-degree-of-freedom maglev vehicle moving on flexible guideways, Journal of Sound and Vibration 235 (2000) 43–61.

[4] X.J. Zheng, J.J. Wu, Y.H. Zhou, Effect of spring non-linearity on dynamic stability of a controlled maglev vehicle and its guideway system, Journal of Sound and Vibration 279 (2005) 201–215.

[5] C.F. Zhao and W.M. Zhai, Maglev vehicle/guideway vertical random response and ride quality, Vehicle System Dynamics 38(3) (2002) 185–210.

[6] J.D. Yau, Vibration control of maglev vehicles traveling over a flexible guideway, Journal of Sound and Vibration 321 (2009a) 184–200.

[7] J.D. Yau, Response of a maglev vehicle moving on a series of guideways with differential settlement, Journal of Sound and Vibration 234 (2009b) 816–831.

[8] J.D. Yau, L. Fryba, Response of suspended beams due to moving loads and vertical seismic ground excitations, Engineering Structures 29 (2007) 3255–3262.

[9] L. Frýba, Vibration of solids and structures under moving loads. 3rd ed., Thomas Telford, London, 1999.

[10] H.M. Irvine, Cable structures, The MIT Press, Cambridge, 1981.

[11] T.T. Soong, Active structural control: theory and practice, Longman Scientific & Technical, Essex, England, 1990.

[12] K.J. Astrom, T. Hagglund, Automatic Tuning of PID Controllers, Instrument Society of America, 1988.

[13] K. Ogata, Modern Control Engineering, third ed., Prentice-Hall International Inc., Englewood Cliffs, NJ, 1997.

[14] Y.B. Yang YB, J.D. Yau, L.C. Hsu, Vibration of simple beams due to trains moving at high speeds, Engineering Structures 19 (1997) 936–944.

[15] J.D. Yau, Y.B. Yang, Vertical accelerations of simple beams due to successive loads traveling at resonant speeds, Journal of Sound and Vibration 289 (2006) 210–228.